European Journal of Pharmaceutics and Biopharmaceutics 72 (2009) 9–17

Contents lists available at ScienceDirect

European Journal of Pharmaceutics and Biopharmaceutics

journal homepage: www.elsevier.com/locate/ejpb

Research paper

Development of new lipid-based paclitaxel nanoparticles using sequential simplex optimization

Xiaowei Dong [a], Cynthia A. Mattingly [a], Michael Tseng [b], Moo Cho [c], Val R. Adams [a], Russell J. Mumper [c,d,*]

[a] Department of Pharmaceutical Sciences, University of Kentucky, USA
[b] Department of Anatomical Science/Neurobiology, University of Louisville, USA
[c] Division of Molecular Pharmaceutics, University of North Carolina at Chapel Hill, NC, USA
[d] UNC Lineberger Comprehensive Cancer Center, University of North Carolina at Chapel Hill, USA

ARTICLE INFO

Article history:
Received 5 August 2008
Revised 14 October 2008
Accepted in revised form 19 November 2008
Available online 10 December 2008

Keywords:
Experimental design
Cancer
Nanocapsule
Cytotoxicity
Lyophilization

ABSTRACT

The objective of these studies was to develop Cremophor-free lipid-based paclitaxel (PX) nanoparticle formulations prepared from warm microemulsion precursors. To identify and optimize new nanoparticles, experimental design was performed combining Taguchi array and sequential simplex optimization. The combination of Taguchi array and sequential simplex optimization efficiently directed the design of paclitaxel nanoparticles. Two optimized paclitaxel nanoparticles (NPs) were obtained: G78 NPs composed of glyceryl tridodecanoate (GT) and polyoxyethylene 20-stearyl ether (Brij 78), and BTM NPs composed of Miglyol 812, Brij 78, and D-alpha-tocopheryl polyethylene glycol 1000 succinate (TPGS). Both nanoparticles successfully entrapped paclitaxel at a final concentration of 150 μg/ml (over 6% drug loading) with particle sizes less than 200 nm and over 85% of entrapment efficiency. These novel paclitaxel nanoparticles were stable at 4 °C over five months and in PBS at 37 °C over 102 h as measured by physical stability. Release of paclitaxel was slow and sustained without initial burst release. Cytotoxicity studies in MDA-MB-231 cancer cells showed that both nanoparticles have similar anticancer activities compared to Taxol®. Interestingly, PX BTM nanocapsules could be lyophilized without cryoprotectants. The lyophilized powder comprised only of PX BTM NPs in water could be rapidly rehydrated with a complete retention of original physicochemical properties, in vitro release properties, and cytotoxicity profile. Sequential Simplex Optimization has been utilized to identify promising new lipid-based paclitaxel nanoparticles having useful attributes.

1. Introduction

Paclitaxel is one of the most effective anticancer agents used in the treatment of various tumors. It is a taxane which interferes with microtubule depolymerization in tumor cells resulting in an arrest of the cell cycle in mitosis followed by the induction of apoptosis. However, the high lattice energy of paclitaxel results in very limited aqueous solubility (approximately 0.7–30 μg/ml) [1,2] contributing to only two commercialized dosage forms of injectable paclitaxel, Taxol®, and Abraxane®. Taxol® is composed of a 50:50 (v/v) mixture of Cremophor EL (polyethoxylated castor oil) and dehydrated alcohol. Serious side effects, such as hypersensitivity reactions, attributable to Cremophor EL have been reported [3]. In clinical therapy, high doses of anti-histamines and gluococorticoids are co-administered to manage these adverse effects, but this strategy has raised the possibility of additional pharmacokinetic and pharmacodynamic issues with paclitaxel. To eliminate Cremophor EL from the paclitaxel formulation, many alternative Cremophor EL-free formulations of paclitaxel have been investigated. Abraxane® is one of those Cremophor EL-free paclitaxel formulations and was registered with the FDA in 2005. Despite its improved clinical profile, Abraxane® is generally not replacing Taxol in cancer chemotherapy, mostly due to its high cost. Therefore, alternative and cost-effective parenteral formulations of paclitaxel are still needed.

Nanoparticles offer an alternative delivery system for cancer therapy that have the potential to control the release rate of drug, improve the drug pharmacokinetics and biodistribution, and reduce drug toxicity. Due to their small size, nanoparticles with entrapped drugs may penetrate tumors due to the discontinuous and leaky nature of the microvasculature of tumors [4,5]. Also, the characteristically poor lymphatic drainage of tumors may result in slower clearance of nanoparticles that accumulate in tumors. This well-known effect is referred to as the enhanced permeability and retention (EPR) effect [6,7].

* Corresponding author. Division of Molecular Pharmaceutics, Center for Nanotechnology in Drug Delivery, UNC Eshelman School of Pharmacy, CB # 7360, University of North Carolina at Chapel Hill, Chapel Hill, NC 27599-7360, USA. Tel.: +1 919 966 1271; fax: +1 919 966 0197.
E-mail address: mumper@email.unc.edu (R.J. Mumper).

0939-6411/$ - see front matter © 2008 Elsevier B.V. All rights reserved.
doi:10.1016/j.ejpb.2008.11.012

Lipid-based particulate delivery systems, including liposomes, micelles, nanocapsules, and solid lipid nanoparticles have been developed especially to solubilize poorly water-soluble and lipophilic drugs. These lipid-based systems have the advantage that comprises bio-derived and/or biocompatible lipids that often result in lower toxicity. In general, the lipid-based systems are made from the combination of lipophilic (oil), amphiphilic (surfactant), and hydrophilic (water) excipients. Formulation approaches typically involve a highly interactive process of experimentally investigating many variables including type and amount of excipients, excipient combinations, and processes (i.e., high-pressure homogenization, microfluidization, extrusion, microemulsion precursors, etc.). Appropriate type and amount of excipients are critical variables, especially in the case of microemulsion precursors to prepare lipid-based systems. Typically, phase diagrams with the blends of different excipients are first developed using the water titration method. Then, combinations of excipients and the drug substance are further optimized for their phase behavior and thermodynamic stability [8,9]. However, when several surfactants and/or oils are used, construction of phase diagrams becomes quite tedious, expensive, and time consuming.

Experimental design is a statistical technique used to simultaneously analyze the influence of multiple factors on the properties of the system being studied. The purpose of experimental design is to plan and conduct experiments in order to extract the maximum amount of information from the collected data in the smallest number of experimental runs. Factorial design based on response surface method has been applied to design formulations [10,11]. However, an increase in the number of factors markedly increases the number of experiments to be carried out. The so-called Taguchi approach proposes a special set of orthogonal arrays to standardize fractional factorial designs [12]. By this approach, the size of the factorial design is reduced. As shown in Fig. 1, sequential simplex optimization is a step-wise strategy for optimization that can adjust many factors simultaneously to rapidly achieve optimal response. The optimization is preceded by moving of a geometric figure (the "simplex"). The starting simplex is composed of $k+1$ vertex (experiments), wherein k is the number of variables. Then, the experiments are performed one by one. The new simplex is obtained based on the results from the previous simplex, and the procedure is repeated until the simplex has rotated and optimum is encircled.

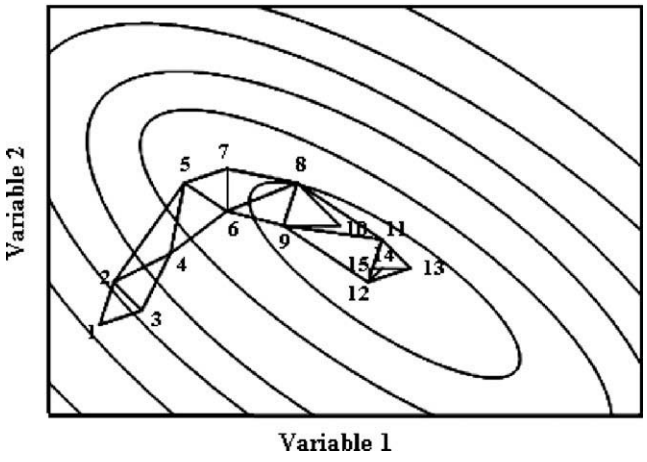

Fig. 1. The principles of sequential simplex optimization for two variables using variable-size simplex rules on the response surface [14]. The starting simplex consists of vertexes 1, 2, and 3 where 1 gives the worst response. The second simplex consists of vertexes 2, 3, and 4 after a reflection and expansion. Finally, the movement of the simplex results in the simplex 12, 14, and 15 which indicates the optimum.

The variable-size simplex algorithm is the modified simplex algorithm which allows the simplex to change its size during movement (Fig. 1). For detailed principles and applications, the reader is referred to the specialized literature [13,14]. Thus, this process of sequential simplex optimization allows for simultaneous formulation development and optimization.

Our laboratory has already reported on the engineering of stable solid lipid-based nanoparticles from oil-in-water (o/w) microemulsion precursors. Nanoparticles (E78 NPs) composed of emulsifying wax (E. wax) as the lipid matrix and Brij 78 as the surfactant were reproducibly prepared with particle sizes less than 150 nm. These E78 NPs were found to have excellent hemocompatibility [15] and were shown to be metabolized in vitro by horse liver alcohol dehydrogenase (HLADH)/NAD^+ [16]. Paclitaxel E78 NPs were shown to overcome Pgp-mediated tumor resistance in vitro in a human HCT-15 colon adenocarcinoma cell line [17] and in vivo in athymic nude mice bearing solid HCT-15 xenograft tumors [18]. However, a shortcoming of the PX E78 NPs used in the above studies was that the entrapment efficiency of paclitaxel in the NPs was only 50%, which resulted in relatively rapid in vitro release (over 80% in 8 h). These shortcomings were directly attributable to the relatively poor solubility of PX in the melted E. Wax.

In light of the above, the objective of these studies was to develop Cremophor-free lipid-based paclitaxel nanoparticle formulations that (1) utilized acceptable oil phases having improved solvation ability for PX, (2) had PX entrapment efficiency >80% with a minimum final concentration of 150 μg/ml with over 5% drug loading, (3) resulted in slow(er) release profiles of PX from NPs, and (4) had a comparable in vitro cytotoxicity to Taxol®. To achieve these objectives, two medium-chain triglycerides, glyceryl tridodecanoate and Miglyol 812, were selected as the oil phases to engineer nanoparticles from o/w microemulsion precursors. Triglycerides are biocompatible/biodegradable excipients [19]. It has been reported that paclitaxel has a high partition coefficient (K_p) in medium-chain triglycerides [20]. Glyceryl tridodecanoate is solid at room temperature, whereas Miglyol 812 is liquid at room temperature. Thus, it was thought that the use of Glyceryl tridodecanoate and Miglyol 812 as oil phases may result in the formation of solid lipid nanoparticles and nanocapsules, respectively. As discussed above, simplex optimization or the combination of Taguchi array and sequential simplex optimization was used to identify optimized systems based on initial response variables (criteria) of particle size and polydispersity index. Identified leads were then fully characterized for stability, entrapment efficiency, in vitro release, and cytotoxicity in human MDA-MB-231 breast cancer cells.

2. Materials and methods

2.1. Materials and cell culture

Paclitaxel, glyceryl tridodecanoate, PBS, and Tween 80 were purchased from Sigma–Aldrich (St. Louis, MO). Emulsifying wax and stearyl alcohol were purchased from Spectrum Chemicals (Gardena, CA). Polyoxyl 20-stearyl ether was obtained from Uniqema (Wilmington, DE). D-Alpha-tocopheryl polyethylene glycol 1000 succinate was purchased from Eastman Chemicals (Kingsport, TN). Miglyol 812 is a mixed caprylic ($C_{8:0}$) and capric ($C_{10:0}$) fatty acid triglyceride and was obtained from Sasol (Witten, Germany). Dialyzers with a molecular weight cutoff (MWCO) of 8000 were obtained from Sigma–Aldrich (St. Louis, MO). Microcon Y-100 with MWCO 100 kDa was purchased from Millipore (Bedford, MA). Ethanol USP grade was purchased from Pharmco-AAPER (Brookfield, CT). Taxol® was obtained from Mayne Pharma Inc. (Paramus, NJ). The human breast cancer cell line, MDA-MB-231, was obtained from American Type Culture Collec-

tion (ATCC) and was maintained in DMEM supplemented with 10% fetal bovine serum (FBS). Cells were cultured at 37 °C in a humidified incubator with 5% CO_2 and maintained in exponential growth phase by periodic subcultivation.

2.2. Preparation of nanoparticles from microemulsion precursors

Nanoparticles were prepared from warm o/w microemulsion precursors as previously described with some modification [21]. Defined amounts of oil phases and surfactants were weighed into glass vials and heated to 65 °C. One (1) ml of filtered and deionized (D.I.) water pre-heated at 65 °C was added into the mixture of melted oils and surfactants. The mixture were stirred for 20 min at 65 °C and then cooled to room temperature. To prepare PX NPs, 150 μg of PX dissolved in ethanol was added directly to the melted oil and surfactant and ethanol was removed by N_2 stream prior to initiating the process described above. Particle size and size distribution of NPs were measured using a N5 Submicron Particle Size Analyzer (Beckman). Ten microliters of nanoparticles was diluted with 1 ml of D.I. water to reach within density range required by the instrument, and particle size analysis was performed at 90° light scattering at 25 °C.

2.3. Development of prototype nanoparticles by sequential simplex optimization

2.3.1. BTM nanoparticles comprised of Miglyol 812, Brij 78, and TPGS

Miglyol 812 and stearyl alcohol were chosen as oil phases, and Brij 78 and TPGS were selected as the surfactants. Taguchi array L-9 (3^4) was first used to help set up the starting simplex for sequential simplex optimization. Particle size and polydispersity index (P.I.) were used to evaluate the results. Three levels for each excipient and Taguchi array are presented in Table 1A. As directed by the results from Taguchi array, the starting simplex was constructed based on the results of trials 3, 5, and 9 with a slight change for each component in each trial (Table 1B). Sequential simplex optimization was then performed as previously described following the variable-size simplex rules [14]. Desirability functions previously developed for the simultaneous optimization of different response variables (criteria) [22] were used to transform response variables (particle size and P.I.) into a measure d (d_{size} or $d_{P.I.}$) that could be adequately compared and combined with each other. Then, the d of the individual response variable was combined into an aggregated value (D value) by using a weighted geometric average. Definitions of d and D value are presented in Eqs. (1) and (2), respectively:

$$d_i = \begin{cases} 0 & Y_i \le a \\ \left[\frac{Y_i - a}{b - a}\right]^s & a < Y_i < b \\ 1 & Y_i \ge b \end{cases} \quad (1)$$

In Eq. (1), i indicates particle size or P.I. The limits were from $a = 70$ nm to $b = 250$ nm for particle size, and from $a = 0.05$ to $b = 1.2$ for P.I. As the optimization in Table 1B was complex, a larger range of P.I. were chosen in order to avoid too many "worst" trials in the simplex, which could stop the optimization. In addition, the larger range of P.I. also helped to seize all possible compositions in the optimization process. For these optimization experiments, particle size and P.I. were given equal importance; thus, the constant $s = 1$.

The overall contribution of all responses is presented as a single aggregated D value as calculated by Eq. (2):

$$D = (d_{\text{particle size}} \times d_{\text{P.I.}})^{1/2} \quad (2)$$

A comparison of each trial in the simplex optimization was based on this aggregated D value which contained information from both particle size and P.I.

After the sequential simplex optimization, Miglyol 812, Brij 78, and TPGS were chosen to form BTM NPs. Four different compositions based on the results from sequential simplex optimization were tested (Table 1C) and were prepared to further optimize BTM NPs.

2.3.2. G78 nanoparticles comprised of glyceryl tridodecanoate and Brij 78

G78 nanoparticles were optimized using MultiSimplex software (CambridgeSoft Corporation, Cambridge, MA). The variable-size simplex rules were also used in this optimization, and response variables included particle size, P.I. and the peak numbers in nanoparticle distribution. The starting simplex was based on our previously optimized E78 NP composition (2 mg E. wax and 4 mg Brij 78 in 1 ml NP suspension). Thus, the limits for particle size and P.I. were naturally smaller than those for the sequential simplex optimization in Section 2.3.1. The limits were from $a = 50$ nm to $b = 200$ nm for particle size, and from $a = 0.01$ to $b = 0.4$ for P.I., and from $a = 1$ to $b = 2$ for peak numbers. Two milliliter NP formulations were prepared for each composition.

2.4. Lyophilization of PX NPs

To determine the effect of lyophilization on the NPs, blank and PX NPs in the presence or absence of 5% lactose were lyophilized using a VirTis® lyophilizer (SP Industries, Gardiner, NY). Two milliliters of each sample was rapidly frozen at −40 °C and then lyophilized using a program of 7.5 h at −10 °C for primary drying and 7.5 h at 25 °C for secondary drying at 100 mTorr. The resultant lyophilized products were reconstituted in 2 ml of D.I. water using a plate shaker for 5 min. The particle sizes of reconstituted lyophilized NPs from six different batches were measured as described above.

2.5. Characterization of paclitaxel G78 and BTM nanoparticles

2.5.1. Particle size and zeta potential measurement

Nanoparticles were analyzed for particle size and size distribution as described above. Ten microliters of blank NPs and PX NPs were diluted with 1 ml of D.I. water plus 10 μl PBS buffer (pH

Table 1A
Taguchi array for the development of BTM nanoparticles. Listed are the compositions per 1 ml nanoparticle suspensions.

Trial	Brij 78 (mg)	TPGS (mg)	Stearyl alcohol (mg)	Miglyol 812 (mg)	Particle size (nm)	P.I.
1	1.6	1.2	0.6	1.4	35	1.21
2	1.6	0.9	0.4	1.0	193.5	0.978
3	**1.6**	**0.6**	**0.2**	**0.6**	**118.4**	**0.159**
4	1.2	1.2	0.4	0.6	25	1.435
5	**1.2**	**0.9**	**0.2**	**1.4**	**212.9**	**0.307**
6	1.2	0.6	0.6	1.0	282.6	0.897
7	0.7	1.2	0.2	1.0	130.5	0.826
8	0.7	0.9	0.6	0.6	315	1.685
9	**0.7**	**0.6**	**0.4**	**1.4**	**234.6**	**0.355**

Bold font indicates promising lead formulations.

Table 1B
Sequential simplex optimization for the development of BTM nanoparticles. Listed are the compositions per 1 ml nanoparticle suspensions.

Trial	Movement	Brij 78 (mg)	TPGS (mg)	Stearyl alcohol (mg)	Miglyol 812 (mg)	Particle size (nm)	P.I.	d_{size}	$d_{P.I.}$	D
1	\	1.6	0.6	0.4	0.6	35.6	0.070	0	0.017	0
2	\	1.2	0.9	0.4	1.4	197.6	0.449	0.709	0.347	0.496
3	\	0.7	0.6	0.8	1.4	186.3	0.360	0.646	0.270	0.417
4	\	1.6	0.9	1.6	1.2	309.2	1.079	0	0.895	0
5	\	0.7	2.1	1.6	1.2	182.7	1.028	0.626	0.85	0.730
6	**R(1, 2, 3, 5)**	**0.5**	**1.2**	**0**	**1.1**	**192.4**	**0.230**	**0.680**	**0.157**	**0.326**

Bold font indicates promising lead formulations.

Table 1C
Development of BTM nanoparticles. Listed are the compositions per 1 ml nanoparticle suspensions.

Trial	Brij 78 (mg)	TPGS (mg)	Miglyol 812 (mg)	Particle size (nm)	P.I.
1	0.5	1.2	1.1	192.4	0.23
2	**1.4**	**0.6**	**1**	**149**	**0.328**
3	0.9	0.6	1.4	190	0.103
4	1.2	1.5	1.2	309.2	1.079

Bold font indicates optimized formulation.

7.4) for the measurement of zeta potential using the Zetasizer Nano Model ZEN2600 (Malvern Instruments, Worcs, UK).

2.5.2. Determination of drug loading and entrapment efficiency

The concentration of PX was quantified by HPLC using a Thermo Finnigan Surveyer HPLC System and an Inertsil ODS-3 column (4.6 × 150 mm) (GL Sciences Inc.) preceded by an Agilent guard column (Zorbax SB-C18, 4.6 × 12.5 mm). The mobile phase was water–acetonitrile (40:60, v/v) at a flow rate of 1.0 ml/min with PX detection at 227 nm. For the paclitaxel standard curve, paclitaxel was dissolved in methanol. To quantify PX in NPs, 1 part of PX NPs in water was dissolved in 8 parts of methanol. PX BTM NPs containing 30% of 7-*epi* PX was dissolved in methanol and then serially diluted in methanol to prepare the standard curve of 7-*epi* PX. Drug loading and entrapment efficiencies were determined by separating free PX from PX-loaded NPs using a Microcon Y-100, and then measuring PX in NP-containing supernatants as described above. To ensure mass balance, the filtrates were also assayed for PX. PX loading and PX entrapment efficiency were calculated as follows:

$$\%\ \text{drug loading} = [(\text{drug entrapped in NPs})/(\text{weight of oil})] \times 100\%\ (\text{w/w})$$

$$\%\ \text{drug entrapment efficiency} = [(\text{drug entrapped in NPs})/(\text{total drug added into NP preparation})] \times 100\%\ (\text{w/w})$$

2.5.3. Particle size stability of NPs in 4 and 37 °C

The physical stability of G78 and BTM nanoparticle suspensions was assessed over storage at 4 °C for five months. Prior to particle size measurement, NP suspensions were allowed to equilibrate to room temperature. The stability of all NP suspensions was also assessed at 37 °C in 10 mM PBS, pH 7.4 by adding 100 μl NP suspensions to 13 ml PBS buffer with a water bath shaker mixing at 150 rpm. At each time interval, 1 ml aliquots were removed and allowed to equilibrate to room temperature prior to particle size measurement.

2.5.4. DSC analysis of G78 NPs

Differential scanning calorimetry (DSC) analysis was performed to determine the physical state of the core (glyceryl tridodecanoate) lipid. Blank G78 or PX G78 nanoparticle suspensions were concentrated about 20-fold using Microcon Y-100 at 4 °C. The concentrated NPs were (1) analyzed by DSC immediately or (2) transferred to an aluminum pan and that was placed in a desiccator for two days at room temperature prior to DSC analysis. As controls, bulk glyceryl tridodecanoate (5 mg), Brij 78 (5 mg) and the bulk mixture of glyceryl tridodecanoate (3.4 mg) and Brij 78 (8 mg) were placed in aluminum pans for DSC analysis (PerkinElmer, Norwalk, CT). Heating curves were recorded using a scan rate of 1 °C/min from 15 to 66 °C.

2.5.5. In vitro release studies

PX release studies (n = 4) were completed at 37 °C by the dialysis method using PBS with 0.1% Tween 80 as a release medium. Before release studies, the solubility of PX in a release medium was measured. Briefly, extra amounts of paclitaxel were added into 2 ml of release medium until saturation was attained. After centrifuge, the concentration of PX in the supernatant was determined by HPLC as described above. For release studies, one milliliter (1 ml) of PX G78 NPs was purified with a Microcon Y-100 and resuspended into 1 ml D.I. water. The concentration of PX in re-suspended PX G78 NPs was measured by HPLC as described above. Eight hundred microliters of purified PX G78 NPs, PX BTM NPs, and reconstituted lyo PX BTM NPs were placed into a regenerated cellulose dialysis membrane (MWCO 8000 Da) submerged in 40 ml PBS with 0.1% Tween 80, respectively, and then shaken in a water bath at a speed of 150 rpm at 37 °C. Free PX was also used as a control. At predetermined times, 200 μl aliquots were taken from outside the dialysis membrane, and replaced with 200 μl fresh media. PX was measured by HPLC as described above. Mass balance was confirmed by measuring PX concentration inside the dialysis membranes after 72 h. In addition, the particle sizes of PX NPs inside the dialysis membranes were measured when release studies were terminated (at 72 h).

2.6. In vitro cytotoxicity studies

The cytotoxicity of PX NPs was tested in human MDA-MB-231 breast cancer cells using the sulforhodamine B (SRB) assay [23]. Cells were seeded into 96-well plates at 1.5×10^4 cells/well and cells were allowed to attach overnight. Cells were incubated for 48 h with drug equivalent concentrations ranging from 10,000 to 0.01 nM for Taxol®, PX-loaded NPs and blank NPs. The SRB assay was performed and IC_{50} values were determined. Briefly, the cell lines were fixed with cold 10% trichloroacetic acid and stained using 0.4% SRB dissolved in 1% acetic acid. The bound dye was solubilized with 10 mM tris base, and the absorbance was measured at 490 nm using a microplate reader. IC_{50} values were calculated

based on the percentage of treatment over control. All groups included three independent experiments ($N = 3$) with triplicates ($n = 3$) for each experiment.

2.7. Statistical analysis

Statistical comparisons were made with ANOVA followed by pair-wise comparisons using Student's *t*-test using GraphPad Prism software. Results were considered significant at 95% confidence interval ($p < 0.05$).

3. Results

3.1. Development of BTM nanoparticles by Taguchi array and sequential simplex optimization

It has previously been reported that a combination of liquid and solid lipid oils enhance drug loading and stability in nanoparticles as compared to only a solid lipid core [24,25]. In the initial development of NPs, a combination oil phase of Miglyol 812 (liquid oil) and stearyl alcohol (solid oil) was selected, in addition to two potential surfactants, Brij 78 and TPGS. Thus, based on these four variables (excipients), Taguchi array was carried out to determine the extent of compositions to which the starting simplex could be formed efficiently. Taguchi's orthogonal array for 3 levels 4 variables (L-9 3^4) is shown in Table 1A. As depicted, trials 3, 5, and 9 gave the most promising results. Thus, the compositions of these three trials (3, 5, and 9) were used to construct the starting simplex in the sequential simplex optimization (Table 1B). As described in the methods section, there were two basic criteria for current nanoparticle formulation: particle size (<200 nm) and P.I. (<0.35). *D* value from desirability functions including particle size and P.I. as response variables was used to evaluate the result of each experiment. Interestingly, the simplex (trial 6 in Table 1B) identified an initial NP formulation that did not contain stearyl alcohol (the solid oil component), but comprises Miglyol 812, Brij 78, and TPGS. Thus, as directed by simplex, subsequent experiments focused on these three excipients. Four different compositions were used to prepare nanoparticles as shown in Table 1C. Among them, trial 2 resulted in optimized NPs having a mean particle size of 149 nm and P.I. of 0.328. Interestingly, due to the relatively low concentration of the resulting NPs, 150 μg/ml of paclitaxel could not be entrapped into these NPs. However, when each component was increased by a factor of 2.5, the more concentrated NP formulation was able to accommodate the desired concentration of PX without changes in particle size and P.I. This final BTM NP formulation consisted of 2.5 mg of Miglyol 812, 1.5 mg of TPGS, and 3.5 mg of Brij 78 in 1 ml water with 150 μg/ml of paclitaxel.

3.2. Development of G78 nanoparticles by sequential simplex optimization

A solid lipid, glyceryl tridodecanoate; was selected as an alternative to lipid-based NPs. Glyceryl tridodecanoate was selected as a possibly direct replacement of E. Wax in the previously described E78 NPs due to the enhanced solubility of PX in glyceryl tridodecanoate. Thus, in this simplex optimization, there were two variables, glyceryl tridodecanoate (oil) and Brij 78 (surfactant). The initial simplex was directed by the MultiSimplex software based on the reference values of 2 mg for glyceryl tridodecanoate and 4 mg for Brij 78 in 1 ml water. Simplex optimization then proceeded as shown in Table 2. After 8 trials, the optimized composition reached nearly constant values in trials 9–11 of 1.6–1.9 mg for glyceryl tridodecanoate and 4–4.2 mg for Brij 78 in 1 ml NP suspension. Finally, trial 11 was identified as the most optimized composition since the composition gave the smallest particle size and the formulation could easily accommodate 150 μg/ml of paclitaxel.

3.3. Lyophilization of BTM and G78 nanoparticles

The lyophilization of blank BTM NPs and PX BTM NPs in water alone resulted in the formation of dry white cakes that were rapidly rehydrated with water within <15 s to produce clear NP suspensions wherein the NPs showed complete retention of original physicochemical properties and in vitro release properties (Figs. 2 and 6). In contrast, lyophilized blank G78 NPs or PX G78 NPs in the presence or absence of 5% lactose as a cryoprotectant could not be rehydrated in water and produced aggregates/agglomerates after rehydration.

3.4. Particle size and zeta potential

All tested nanoparticles had mean particle size diameters less than 200 nm with zeta potentials of about −6 mV regardless of PX entrapment. The entrapment of paclitaxel had no influence on the mean particle size of G78 and BTM nanoparticles (Table 3). Interestingly, rehydrated lyophilized NPs had smaller particle sizes for both blank BTM NPs and PX BTM NPs (Fig. 2).

3.5. Drug loading and entrapment efficiencies of paclitaxel in nanoparticles

HPLC analysis showed that the 7-*epi* isomer of PX was present at about 30% when PX was formulated in NPs in water. Further analysis showed that the epimerization occurred during the preparation of the PX NPs [26]. However, epimerization at C7 is reversible and can be prevented by forming PX NPs at slightly acidic pH [27]. 7-*epi* isomer of PX did not form when PX BTM NPs were prepared in 10% lactose (pH 5) or 50 mM sodium acetate buffer (pH 6). The slope of the standard curve for 7-*epi* PX was not statistically different from that for PX (data not shown). Thus, the standard curve for PX was used to determine the total PX concentration (PX plus 7-*epi* PX).

The entrapment efficiencies for PX G78 NPs and PX BTM NPs were 85% and 97.5% as shown in Table 3. The mass balance of PX was 85.4 ± 3.3% and 97.5 ± 2.6% (mean ± SD, $n = 3$) for PX G78 NPs and PX BTM NPs, respectively. The results showed that paclitaxel was incorporated into nanoparticles at weight ratio of over 6% of the selected lipid core. Finally, rehydrated lyophilized PX BTM NPs showed 93.1% of entrapment efficiency, which was not statistically different to that of non-lyophilized PX BTM NPs ($p > 0.05$).

3.6. Physical stability of nanoparticles

The physical stability of paclitaxel nanoparticles was evaluated by monitoring changes of particle sizes at 4 °C upon long-term storage as well as short-term stability at 37 °C in PBS to simulate physiological conditions. The particle sizes of G78 and BTM nanoparticles with or without paclitaxel did not significantly change at 4 °C for five months (Fig. 3). To test stability of nanoparticles in physiological conditions, G78 NPs, BTM NPs, and reconstituted lyophilized BTM NPs were incubated in PBS at 37 °C for 102 h. Particle sizes of PX-loaded and blank nanoparticles slightly increased after 72 h incubation. The data for PX-loaded NPs are shown in Fig. 4, whereas the data for blank NPs are not shown.

3.7. Physical state of the core lipid in G78 nanoparticles

It has been reported that glyceryl tridodecanoate (also called "trilaurin") existed as super-cooled melts rather than in a solid

Table 2
Simplex optimization for the development of G78 nanoparticles. Listed are the compositions per 1 ml nanoparticle suspensions.

Trial	Brij 78 (mg)	Glyceryl tridodecanoate (mg)	Particle size (nm)	P.I.	Peak #[a]	Current membership[b]
1	3.5	1.5	157.2	0.3	2	0
2	4.5	1.8	153.5	0.36	1	4.77E−02
3	3.8	2.5	194.6	0.275	1	1.73E−02
4	4.8	2.8	195.3	0.25	2	0
5*	3.8	1.8	161.9	0.258	1	0.138
6	4.5	1.1	–[c]	–	–	–
7	4.0	2.1	199	0.282	1	3.03E−03
8	3.3	2.2	–	–	–	–
9*	4.2	1.9	161.3	0.274	1	0.125
10	4.0	1.6	156.4	0.325	1	8.38E−02
11*	**4.0**	**1.7**	**143.6**	**0.369**	**1**	**4.48E−02**

Bold font indicates optimized formulation.
* indicates the composition of the final simplex.
[a] The peak numbers in nanoparticle distribution.
[b] Current membership has the same meaning and definition with *D* value in desirability functions.
[c] Impossible to form nanoparticles based on this composition.

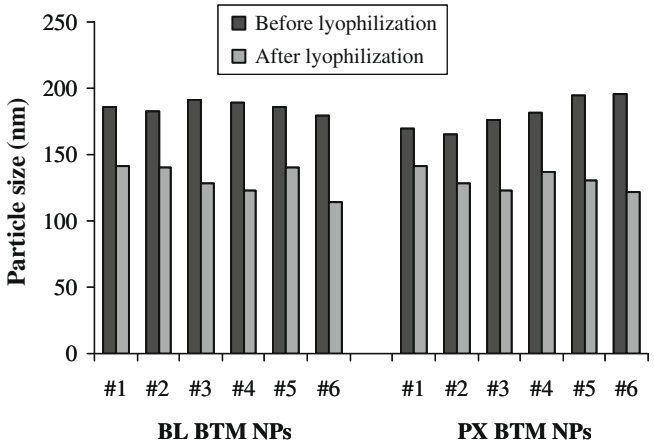

Fig. 2. Particle size of BTM nanoparticles before and after lyophilization (and rehydration). Six different batches were tested for both blank BTM nanoparticles and PX-loaded BTM nanoparticles. For all tested NP formulations, P.I. values ranged from 0.03 to 0.35 indicating uniform, mono-dispersed NPs. Data are presented as the mean particle size of three separate measurements of each batch.

state in nanoparticles [28,29]. Thus, in the present studies, DSC analysis was used to determine the physical state of glyceryl tridodecanoate in G78 nanoparticles. Bulk glyceryl tridodecanoate showed the melting peak at 46 °C while Brij 78 had two melting peaks at 35 and 40 °C. The concentrated blank and PX G78 NPs clearly showed an endothermal peak at 43 °C (Fig. 5B). After drying of the NPs, two other peaks at 35 and 40 °C appeared for blank or PX G78 NPs (Fig. 5A). The endothermal peaks of Brij 78 intensified after drying suggesting that more Brij 78 existed in the solid state. The melting peak of glyceryl tridodecanoate in nanoparticles shifted to lower temperature and broader compared to that of bulk material. However, the endothermic peak at 43 °C for glyceryl tridodecanoate indicated that glyceryl tridodecanoate retained a solid state in G78 nanoparticles.

3.8. In vitro release of paclitaxel from nanoparticles

Paclitaxel has been reported to have aqueous solubility of 0.7–30 μg/ml. Therefore, to maintain sink conditions, PBS with 0.1% Tween 80 was used as the release medium for the in vitro release studies of paclitaxel. The solubility of paclitaxel in the release medium at room temperature was 10.8 ± 0.3 μg/ml (mean ± SD, $n = 3$) as measured by HPLC. Thus, for the release studies, 800 μl of PX NPs containing 150 μg/ml of paclitaxel was placed into 40 ml of the release medium. There was no 7-*epi* PX observed during the release study of free paclitaxel. The cumulative release of paclitaxel from PX NPs was calculated based on the total PX (PX plus 7-*epi* PX) released, and is shown in Fig. 6. Free PX was released completely within 4 h. For all tested PX NPs, although the initial release rates were greater between 0 and 8 h, no initial burst of PX was observed. After 8 h, the release rates were much lower. The results showed that the mean cumulative release of PX after 72 h was 40%, 50%, and 53% from PX G78 NPs, PX BTM NPs, and reconstituted lyophilized PX BTM NPs, respectively. Mass balance analysis for PX G78 NPs, PX BTM NPs, and lyophilized PX NPs showed that 79.2 ± 8.6%, 98.3 ± 24.2%, and 73.4 ± 16.6% (mean ± SD, $n = 4$) of the PX was recovered, respectively. There were no other PX degradation peaks, except for 7-*epi* PX, observed by HPLC during the course of the studies. Moreover, lyophilized PX BTM NPs showed the same release profile as compared to PX BTM NPs ($p > 0.05$ at each time point). Also, the particle sizes of all tested nanoparticles did not change significantly after 72 h.

3.9. In vitro cytotoxicity studies

The cytotoxicity of PX NPs was tested in human breast cancer MDA-MB-231 cells using the SRB assay (Table 4). PX NPs showed a clear dose-dependent cytotoxicity in MDA-MB-231 cells. There was no statistical significance in the IC_{50} values of PX BTM NPs and lyophilized PX BTM NPs compared to commercial Taxol®. However, the IC_{50} of PX G78 NPs had comparable but statistically different IC_{50} values compared to Taxol®. Blank NPs showed some cytotoxicity but only the paclitaxel equivalent dose of 617.3 and 354.6 nM of PX which corresponds to a total NP concentration of 26.4 and 15.1 μg/ml for blank G78 NPs and BTM NPs, respectively.

4. Discussion

Paclitaxel is an important agent in the treatment of metastatic breast cancer. However, the optimal clinical use of paclitaxel is limited due to its poor aqueous solubility. Commercial paclitaxel formulation, Taxol®, is generally associated with hypersensitivity reactions which results from the excipient Cremophor EL in Taxol®. To overcome the problems, numerous lipid-based and Cremophor EL-free paclitaxel formulations have been investigated, such as liposomes [30], solid lipid nanoparticles [31,32], micelles [33,34], emulsions [35,36].

In the present study, two median chain triglycerides, glyceryl tridodecanoate and Miglyol 812, were used to investigate new li-

Table 3
Physiochemical properties of PX G78, PX BTM, and lyo PX BTM nanoparticles ($n = 3$).

Formulations	Theoretical loading (μg/ml)	Mean[a] diameter (nm)	P.I.	Zeta potential (mV)	% Drug loading (w/w, drug/oil)	% Drug entrapment efficiency
PX G78NPs	150	169.2 ± 8.1	0.302 ± 0.027	−6.6 ± 2.6	7.5	85.4 ± 3.3
PX BTM NPs	150	190.5 ± 7.8	0.279 ± 0.054	−5.9 ± 1.78	6	97.5 ± 2.6[#]
Lyo PX BTM NPs	150	130.0 ± 7.8	0.284 ± 0.042	−5.1 ± 1.00	6	93.1 ± 4.1[#]

[a] The data are presented as the mean of the mean particle size of nanoparticles in different batches ±SD ($n = 3$).
[#] $p > 0.05$.

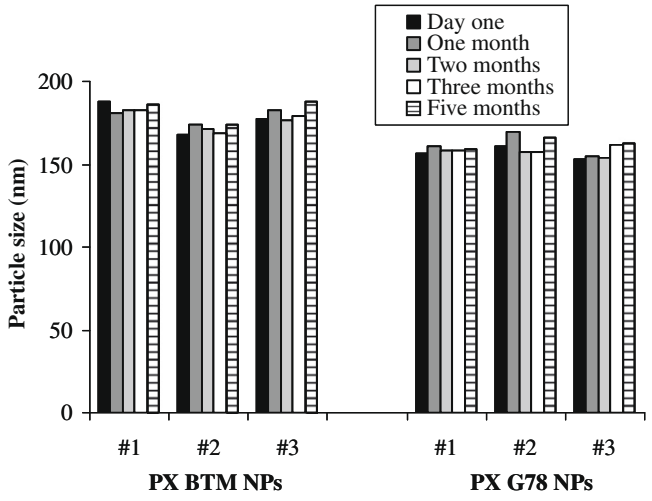

Fig. 3. Long-term stability of paclitaxel nanoparticles stored at 4 °C. Three different batches of PX-loaded BTM and G78 nanoparticles were monitored for particle sizes over five months. For all tested samples, P.I. < 0.35. Data are presented as the mean particle size of three separate measurements of each batch.

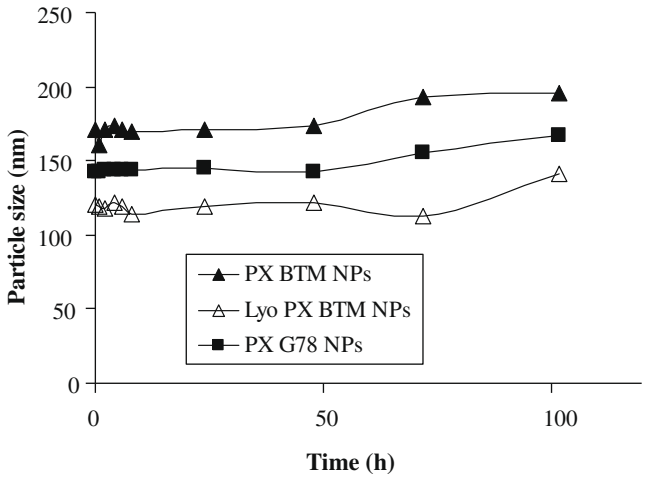

Fig. 4. Stability of paclitaxel nanoparticles in PBS at 37 °C. PX BTM nanoparticles, reconstituted lyophilized PX BTM nanoparticles and PX G78 nanoparticles were monitored for particle sizes for 102 h. For all tested samples, P.I. < 0.35. Data are presented as the mean particle size of three separate measurements of each batch.

pid-based nanoparticles for paclitaxel. Relative to other candidate oil phases, these two oils have high solvation ability for PX. Glyceryl tridodecanoate has a relatively low melting point of 46 °C, which theoretically facilitates the preparation of lower crystalline cores which may accommodate a greater concentration of drug [25]. Miglyol 812, being a liquid, forms a reservoir-type drug delivery system in which poorly water-soluble drugs remain dissolved inside the liquid oil core and consequently a high payload and reduced release profile may be achieved [37,38]. As expected, the final optimized nanoparticles, G78 NPs and BTM NPs, successfully entrapped paclitaxel with high loading and entrapment efficiency (Table 3). However, the selection of these two alternative oil phases required the development of optimized NP formulations. To facilitate, we used a methodology that combined Taguchi array and sequential simplex optimization. The simplex is made of $k + 1$ vertex. The response of the experiment in each vertex is ranked and the "worst" response is replaced by the new set of variables for the next experiment. To efficiently move the simplex, there should be limited "worst" responses in the staring simplex. As new excipients were investigated and no prior compositions were used as a reference (Table 1), Taguchi array was first performed to explore and provide the framework of the starting simplex. The final optimization was then completed using sequential simplex optimization. Trial 6 in Table 1B identified a new nanoparticle formulation composed of the liquid oil Miglyol 812. After further optimization, new BTM nanoparticles were developed. In the case of G78 NPs, it closely resembled the previously developed E78 NPs (Table 2); thus, the sequential simplex optimization was directly used for the investigation of G78 NPs. The results for both PX NPs indicate that this new methodology combining Taguchi array and sequential simplex optimization could efficiently and effectively be used to identify optimized nanoparticles. Finally, a total of 19 trials and 11 trials were used to obtain optimized BTM NPs and G79 NPs, respectively. In contrast, even for 4 factors and 3 levels design, e.g., optimization in Tables 1A and 1B, complete factorial design would require $3^4 = 81$ experiments. To our best knowledge, this is the first report to use the combination of Taguchi array and sequential simplex optimization for the development of nanoparticles.

Choosing appropriate lipids could help increase the entrapment efficiency of drug and slow the release rate of the drug from the nanoparticles. As compared with PX E78 NPs previously developed in our laboratory, the optimal PX BTM and G78 nanoparticles were very reproducible with high drug loading and showed much slower release of PX achieving about 50% and 40% after 72 h, respectively (Fig. 6). The slow and sustained release of paclitaxel without burst release from PX BTM and PX G78 nanoparticles indicated that paclitaxel was likely not present at or near the surface of nanoparticles but instead within the core of the NPs as ideally predicted by the enhanced solvation ability of Miglyol 812 and glyceryl tridodecanoate for PX. Moreover, entrapment of paclitaxel into nanoparticles did not change the sizes of nanoparticles. All PX NPs had particle sizes less than 200 nm, even after 102 h of incubation in PBS at 37 °C. These data indicate potential stability of PX NPs in vivo after intravenous injection (Fig. 4). Cytotoxicity studies showed that both PX G78 and BTM nanoparticles had the same or comparable anticancer activity compared to commercial Taxol® in human MDA-MB-231 breast cancer cells. Therefore, both of these identi-

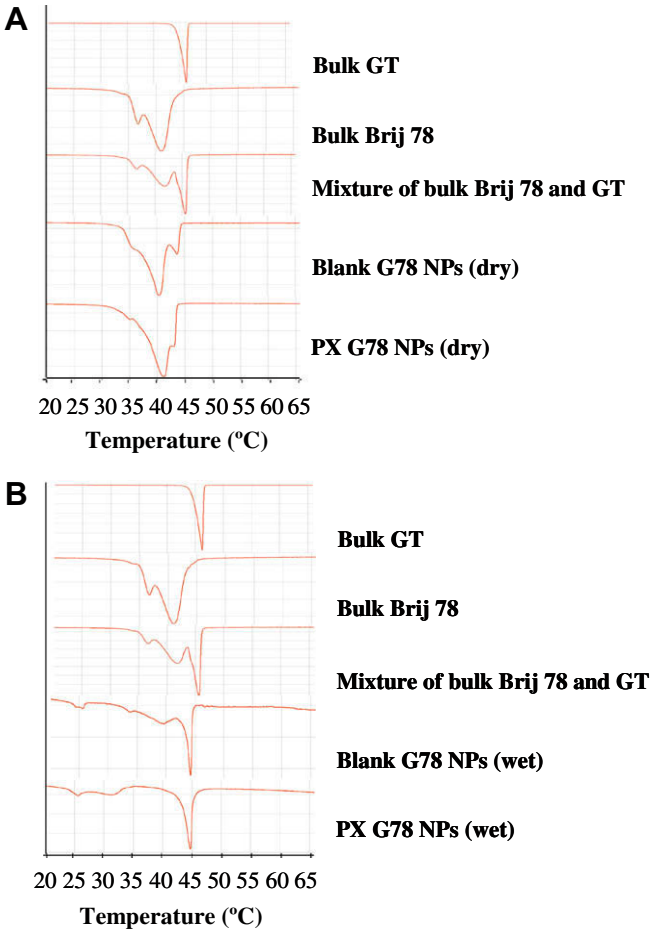

Fig. 5. DSC of G78 nanoparticles. (A) The concentrated nanoparticles were dried by desiccation for two days prior to DSC analysis ("dry"). (B) DSC analysis of nanoparticles was performed immediately after concentrating nanoparticles ("wet"). GT means glyceryl tridodecanoate.

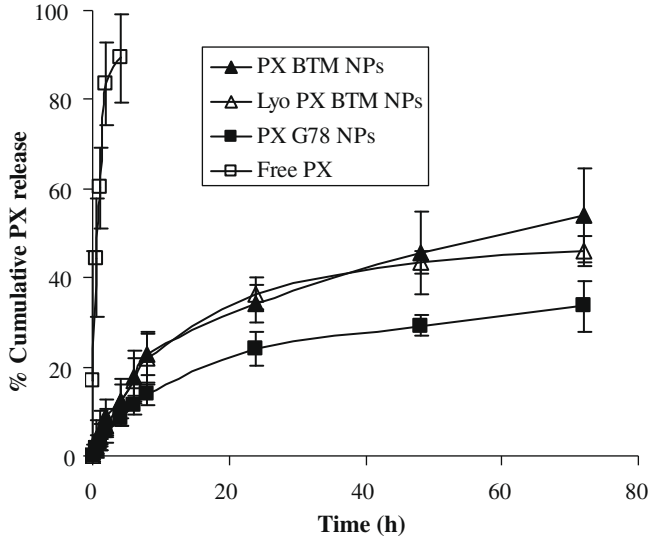

Fig. 6. Release of PX from PX nanoparticles at 37 °C. Paclitaxel release was measured using the dialysis method in PBS (pH 7.4) with 0.1% Tween 80 as described in Section 2. Data are presented as the mean ± SD (n = 4).

fied PX NP formulations may be good candidates for ligand-mediated tumor-targeted delivery of PX.

Several studies have reported that glyceryl tridodecanoate is retained in lipid-based NPs in a super-cooled liquid state. If true, this semi-stable state of glyceryl tridodecanoate will likely affect the stability of nanoparticles due to the predicted phase transition of the super-cooled core to the crystalline phase. However, the present studies showed using DSC analysis that glyceryl tridodecanoate remained as a solid state in G78 NPs (Fig. 5), suggesting that the phenomenon of super-cooled glyceryl tridodecanoate in nanoparticles may be dependent on the process and compositions (i.e., surfactant) used to prepare the nanoparticles. Blank and PX G78 nanoparticles stored as liquid suspensions at 4 °C remained stable for several months and exhibited no change in particle size. There was some concern that G78 nanoparticles, made with the lower melting GT, may be adversely affected by body temperature. However, either blank or PX G78 nanoparticles showed no change in particle sizes after 102 h of incubation in PBS at 37 °C.

It is thought that BTM NPs may be a novel liquid reservoir, or nanocapsule-type formulation. The liquid reservoir containing paclitaxel dissolved in Miglyol 812 is stabilized with the polymeric surfactants Brij 78 and TPGS. Higher drug loading of PX BTM nanoparticles indicates the advantage of this nanocapsule-type formulation as compared to the solid-core type G78 NP system. The BTM NPs were spontaneously formed after cooling from the warm o/w microemulsion precursors. It is thought that the BTM NPs are nanocapsules and not nanoemulsions since nanoemulsions are non-equilibrium and thermodynamically unstable systems that cannot, by definition, form spontaneously without agitation or significant mechanical/shear mixing [39]. Another very interesting discovery was serendipitously made during the course of the present studies. In one attempt to concentrate NP formulations to analyze for entrapped PX, NPs were lyophilized in water. The BTM NP formulations produced uniform white cakes that could be rapidly rehydrated with complete retention of original physicochemical properties, in vitro release properties, and cytotoxicity profile. Our experience, as well as others, is that it is often difficult to freeze-dry colloidal suspensions in the presence of cryoprotectants. To our knowledge, there are few or no reports on the successful lyophilization of colloidal suspensions without the use of a cryoprotectant which protects the nanoparticles from the stresses of the freezing and thawing process. Moreover, the lyophilization of nanoemulsions or nanocapsules is thought to be even more challenging due to the existence of the very thin and fragile lipid envelope that may not withstand the mechanical stress of freezing [40,41]. Even in the presence of cryoprotectants, an increase of particle size is likely to occur [42]. In the present studies, the optimal BTM nanoparticles were successfully lyophilized without cryoprotectants. The non-collapsed uniform cakes of PX BTM NPs in water alone were rehydrated and spontaneously produced particle sizes that were, in fact, slightly smaller than the original particle sizes. In addition, there was a complete retention of the in vitro release properties and cytotoxicity profile.

In conclusion, the combination of Taguchi array and sequential simplex optimization efficiently guided the development and optimization of lipid-based nanoparticulate formulation for paclitaxel. Injectable paclitaxel nanoparticles, PX G78 NPs and PX BTM NPs, were successfully prepared via a warm o/w microemulsion precursor engineering method. Both paclitaxel nanoparticle suspensions were physically stable at 4 °C over five months, and PX BTM could be lyophilized without cryoprotectants. PX G78 and BTM nanoparticles showed comparable or same anticancer activity compared to Taxol® in MDA-MB-231 breast cancer cells. Therefore, these paclitaxel-loaded nanoparticles may be candidates for ligand-mediated tumor-targeted delivery of paclitaxel after intravenous injection.

Table 4
IC_{50} values of paclitaxel nanoparticles in MDA-MB-231 cells at 48 h.

Formulations	Taxol®	G78 NPs		BTM NPs #1		BTM NPs #2[a]		Lyo BTM NPs #2[a]	
		PX NPs[*]	BL NPs	PX NPs[#]	BL NPs[##]	PX NPs[#]	BL NPs[##]	PX NPs[#]	BL NPs[##]
IC_{50} (nM)	7.2 ± 2.9	21.0 ± 1.5	617.3 ± 356	7.6 ± 1.2	354.6 ± 59.0	15.1 ± 6.8	342.7 ± 119.6	15.6 ± 10.6	256.1 ± 128.6

Data are presented as the mean ± SD of three independent experiments ($N = 3$) with triplicate ($n = 3$) measurements for each sample/concentration tested.
[a] Lyo BTM NPs #2 were directly lyophilized from BTM NPs #2. Lyophilized powder was stored at 4 °C for overnight prior to completing the cytotoxicity studies.
[#] $p > 0.05$ compared to IC_{50} of Taxol®.
[##] $p > 0.05$ within the group.
[*] $p < 0.05$ compared to IC_{50} of Taxol®.

Acknowledgment

This research was supported by NIH-NCI R01 CA115197 to R.J.M., V.A., and M.T.

References

[1] A.E. Mathew, M.R. Mejillano, J.P. Nath, R.H. Himes, V.J. Stella, Synthesis and evaluation of some water-soluble prodrugs and derivatives of taxol with antitumor activity, J. Med. Chem. 35 (1) (1992) 145–151.
[2] C.S. Swindell, N.E. Krauss, Biologically active taxol analogues with deleted A-ring side chain substituents and variable C-2′ configuration, J. Med. Chem. 34 (1991) 1176–1184.
[3] R.B. Weiss, R.C. Donehower, P.H. Wiernik, T. Ohnuma, R.J. Gralla, D.L. Trump, J.R. Baker Jr., D.A. Van Echo, D.D. Von Hoff, B. Leyland-Jones, Hypersensitivity reactions from taxol, J. Clin. Oncol. 8 (7) (1990) 1263–1268.
[4] R. Pasqualini, W. Arap, D.M. McDonald, Probing the structural and molecular diversity of tumor vasculature, Trends Mol. Med. 8 (12) (2002) 563–571.
[5] S.K. Hobbs, W.L. Monsky, F. Yuan, W.G. Roberts, L. Griffith, V.P. Torchilin, R.K. Jain, Regulation of transport pathways in tumor vessels: role of tumor type and microenvironment, Proc. Natl. Acad. Sci. USA 95 (8) (1998) 4607–4612.
[6] F.M. Muggia, Doxorubicin–polymer conjugates: further demonstration of the concept of enhanced permeability and retention, Clin. Cancer Res. 5 (1) (1999) 7–8.
[7] H. Maeda, T. Sawa, T. Konno, Mechanism of tumor-targeted delivery of macromolecular including the drugs EPR effect in solid tumor and clinical overview of the prototype polymeric drug SMANCS, J. Control Release 74 (1–3) (2001) 47–61.
[8] B.K. Kang, J.S. Lee, S.K. Chon, S.Y. Jeong, S.H. Yuk, G. Khang, H.B. Lee, S.H. Cho, Development of self-microemulsifying drug delivery systems (SMEDDS) for oral bioavailability enhancement of simvastatin in beagle dogs, Int. J. Pharm. 274 (1–2) (2004) 65–73.
[9] P.M. Bummer, Physical chemical considerations of lipid-based oral drug delivery – solid lipid nanoparticles, Crit. Rev. Ther. Drug Carrier Syst. 21 (1) (2004) 1–20.
[10] M.C. Gohel, A.F. Amin, Formulation optimization of controlled release diclofenac sodium microspheres using factorial design, J. Control Release 51 (2–3) (1998) 115–122.
[11] M.D. Bhavsar, S.B. Tiwari, M.M. Amiji, Formulation optimization for the nanoparticles-in-microsphere hybrid oral delivery system using factorial design, J. Control Release 110 (2) (2006) 422–430.
[12] R.K. Roy, Design of Experiments using the Taguchi Approach, John Wiley & Sons, Inc., New York, NY, 2001.
[13] J. Gabrielsson, N. Lindberg, T. Lundstedt, Multivariate methods in pharmaceutical applications, J. Chemometrics 16 (2002) 141–160.
[14] F.H. Walters, L.R. Parker, S.L. Morgan, S.N. Deming, Sequential Simplex Optimization, CRC Press Inc., Boca Raton, FL, 1991.
[15] J.M. Koziara, J.J. Oh, W.S. Akers, S.P. Ferraris, R.J. Mumper, Blood compatibility of cetyl alcohol/polysorbate-based nanoparticles, Pharm. Res. 22 (11) (2005) 1821–1828.
[16] X. Dong, R.J. Mumper, The metabolism of fatty alcohols in lipid nanoparticles by alcohol dehydrogenase, Drug Dev. Ind. Pharm. 32 (8) (2006) 973–980.
[17] J.M. Koziara, P.R. Lockman, D.D. Allen, R.J. Mumper, Paclitaxel nanoparticles for the potential treatment of brain tumors, J. Control Release 99 (2) (2004) 259–269.
[18] J.M. Koziara, T.R. Whisman, M.T. Tseng, R.J. Mumper, In-vivo efficacy of novel paclitaxel nanoparticles in paclitaxel-resistant human colorectal tumors, J. Control Release 112 (3) (2006) 312–319.
[19] K.A. Traul, A. Driedger, D.L. Ingle, D. Nakhasi, Review of the toxicologic properties of medium-chain triglycerides, Food Chem. Toxicol. 38 (1) (2000) 79–98.
[20] A.B. Dhanikula, N.M. Khalid, S.D. Lee, R. Yeung, V. Risovic, K.M. Wasan, J.C. Leroux, Long circulating lipid nanocapsules for drug detoxification, Biomaterials 28 (6) (2007) 1248–1257.
[21] M.O. Oyewumi, R.J. Mumper, Gadolinium-loaded nanoparticles engineered from microemulsion templates, Drug Dev. Ind. Pharm. 28 (3) (2002) 317–328.
[22] G. Derringer, R. Suich, Simultaneous optimization of several response variables, J. Qual. Tech. 12 (1980) 214–219.
[23] K.T. Papazisis, G.D. Geromichalos, K.A. Dimitriadis, A.H. Kortsaris, Optimization of the sulforhodamine B colorimetric assay, J. Immunol. Methods 208 (1997) 151–158.
[24] R.H. Muller, M. Radtke, S.A. Wissing, Nanostructured lipid matrices for improved microencapsulation of drugs, Int. J. Pharm. 242 (1–2) (2002) 121–128.
[25] K. Manjunath, J.S. Reddy, V. Venkateswarlu, Solid lipid nanoparticles as drug delivery systems, Methods Find. Exp. Clin. Pharmacol. 27 (2) (2005) 127–144.
[26] G.J. MacEachern-Keith, L.J. Wagner Butterfield, M.J. Incorvia Mattina, Paclitaxel stability in solution, Anal. Chem. 69 (1997) 72–77.
[27] J. Tian, V.J. Stella, Degradation of paclitaxel and related compounds in aqueous solutions I: epimerization, J. Pharm. Sci. 97 (3) (2008) 1224–1235.
[28] H. Bunjes, K. Westesen, M.H.J. Koch, Crystallization tendency and polymorphic transitions in triglyceride nanoparticles, Int. J. Pharm. 129 (1996) 159–173.
[29] B. Siekmann, K. Westesen, Thermoanalysis of the recrystallization process of melt-homogenized glyceride nanoparticles, Colloids Surf. B Biointerfaces 3 (1994) 159–175.
[30] J.A. Zhang, G. Anyarambhatla, L. Ma, S. Ugwu, T. Xuan, T. Sardone, I. Ahmad, Development and characterization of a novel Cremophor EL free liposome-based paclitaxel (LEP-ETU) formulation, Eur. J. Pharm. Biopharm. 59 (1) (2005) 177–187.
[31] M.K. Lee, S.J. Lim, C.K. Kim, Preparation characterization and in vitro cytotoxicity of paclitaxel-loaded sterically stabilized solid lipid nanoparticles, Biomaterials 28 (12) (2007) 2137–2146.
[32] L.E. van Vlerken, Z. Duan, M.V. Seiden, M.M. Amiji, Modulation of intracellular ceramide using polymeric nanoparticles to overcome multidrug resistance in cancer, Cancer Res. 67 (10) (2007) 4843–4850.
[33] M. Sznitowska, M. Klunder, M. Placzek, Paclitaxel solubility in aqueous dispersions and mixed micellar solutions of lecithin, Chem. Pharm. Bull. 56 (1) (2008) 70–74.
[34] S. Hassan, S. Dhar, M. Sandstrom, D. Arsenau, M. Budnikova, I. Lokot, N. Lobanov, M.O. Karlsson, R. Larsson, E. Lindhagen, Cytotoxic activity of a new paclitaxel formulation, Pacliex, in vitro and in vivo, Cancer Chemother. Pharmacol. 55 (1) (2005) 47–54.
[35] P. Kan, Z.B. Chen, C.J. Lee, I.M. Chu, Development of nonionic surfactant/phospholipid o/w emulsion as a paclitaxel delivery system, J. Control Release 58 (3) (1999) 271–278.
[36] P.P. Constantinides, K.J. Lambert, A.K. Tustian, B. Schneider, S. Lalji, W. Ma, B. Wentzel, D. Kessler, D. Worah, S.C. Quay, Formulation development and antitumor activity of a filter-sterilizable emulsion of paclitaxel, Pharm. Res. 17 (2) (2000) 175–182.
[37] M. Fresta, G. Cavallaro, G. Giammona, E. Wehrli, G. Puglisi, Preparation and characterization of polyethyl-2-cyanoacrylate nanocapsules containing antiepileptic drugs, Biomaterials 17 (8) (1996) 751–758.
[38] V.C. Mosqueira, P. Legrand, H. Pinto-Alphandary, F. Puisieux, G. Barratt, Poly(D,L-lactide) nanocapsules prepared by a solvent displacement process: influence of the composition on physicochemical and structural properties, J. Pharm. Sci. 89 (5) (2000) 614–626.
[39] C. Solans, P. Izquierdo, J. Nolla, N. Azemar, M.J. Garacia-Celema, Nano-emulsions, Curr. Opin. Colloid Interface Sci. 10 (2005) 102–110.
[40] S.R. Schaffazick, A.R. Pohlmann, T. Dalla-Costa, S.S. Guterres, Freeze-drying polymeric colloidal suspensions: nanocapsules, nanospheres and nanodispersion. A comparative study, Eur. J. Pharm. Biopharm. 56 (3) (2003) 501–505.
[41] W. Abdelwahed, G. Degobert, H. Fessi, A pilot study of freeze drying of poly(epsilon-caprolactone) nanocapsules stabilized by poly(vinyl alcohol): formulation and process optimization, Int. J. Pharm. 309 (1–2) (2006) 178–188.
[42] B. Heurtault, P. Saulnier, B. Pech, J.E. Proust, J.P. Benoit, A novel phase inversion-based process for the preparation of lipid nanocarriers, Pharm. Res. 19 (6) (2002) 875–880.